

THE CONNECTION BETWEEN GAMMA-RAY BURSTS AND EXTREMELY METAL-POOR STARS: BLACK HOLE-FORMING SUPERNOVAE WITH RELATIVISTIC JETS

NOZOMU TOMINAGA¹, KEIICHI MAEDA², HIDEYUKI UMEDA¹, KEN'ICHI NOMOTO^{1,3}, MASAOMI TANAKA¹,
NOBUYUKI IWAMOTO⁴, TOMOHARU SUZUKI¹, AND PAOLO A. MAZZALI^{1,5,6}

Accepted for publication in the Astrophysical Journal Letters (10 March 2007, v657n2 issue).

ABSTRACT

Long-duration gamma-ray bursts (GRBs) are thought to be connected to luminous and energetic supernovae (SNe), called hypernovae (HNe), resulting from the black-hole (BH) forming collapse of massive stars. For recent nearby GRBs 060505 and 060614, however, the expected SNe have not been detected. The upper limits to the SN brightness are about 100 times fainter than GRB-associated HNe (GRB-HNe), corresponding to the upper limits to the ejected ⁵⁶Ni masses of $M(^{56}\text{Ni}) \sim 10^{-3}M_{\odot}$. SNe with a small amount of ⁵⁶Ni ejection are observed as faint Type II SNe. HNe and faint SNe are thought to be responsible for the formation of extremely metal-poor (EMP) stars. In this Letter, a relativistic jet-induced BH forming explosion of the 40 M_{\odot} star is investigated and hydrodynamic and nucleosynthetic models are presented. These models can explain both GRB-HNe and GRBs without bright SNe in a unified manner. Their connection to EMP stars is also discussed. We suggest that GRBs without bright SNe are likely to synthesize $M(^{56}\text{Ni}) \sim 10^{-4}$ to $10^{-3}M_{\odot}$ or $\sim 10^{-6}M_{\odot}$.

Subject headings: Galaxy: halo — gamma rays: bursts — nuclear reactions, nucleosynthesis, abundances — stars: abundances — stars: Population II — supernovae: general

1. INTRODUCTION

Long-duration gamma-ray bursts (GRBs) at sufficiently close distances ($z < 0.2$) have been found to be accompanied by luminous and energetic Type Ic supernovae (SNe Ic) called hypernovae (HNe; GRB 980425/SN 1998bw: Galama et al. 1998; GRB 030329/SN 2003dh: Stanek et al. 2003, Hjorth et al. 2003; GRB 031203/SN 2003lw: Malesani et al. 2004). These GRB-associated HNe (GRB-HNe) are suggested to be the outcome of very energetic black hole (BH) forming explosions of massive stars (e.g., Iwamoto et al. 1998). The ejected ⁵⁶Ni mass is estimated to be $M(^{56}\text{Ni}) \sim 0.3 - 0.7M_{\odot}$ (e.g., Mazzali et al. 2006) which is 4 – 10 times larger than typical SNe Ic [$M(^{56}\text{Ni}) \sim 0.07M_{\odot}$; Nomoto et al. 2006b].

For recently discovered nearby long-duration GRB 060505 ($z = 0.089$, Fynbo et al. 2006) and GRB 060614 ($z = 0.125$, Gal-Yam et al. 2006; Fynbo et al. 2006; Della Valle et al. 2006; Gehrels et al. 2006), no SN was detected.⁷ Upper limits to brightness of the possible SNe are about 100 times fainter than SN 1998bw [i.e., $M(^{56}\text{Ni}) \lesssim 10^{-3}M_{\odot}$].

¹ Department of Astronomy, School of Science, University of Tokyo, Bunkyo-ku, Tokyo, Japan; tominaga@astron.s.u-tokyo.ac.jp

² Department of Earth Science and Astronomy, Graduate School of Arts and Science, University of Tokyo, Tokyo, Japan

³ Research Center for the Early Universe, School of Science, University of Tokyo, Bunkyo-ku, Tokyo, Japan

⁴ Nuclear Data Center, Nuclear Science and Engineering Directorate, Japan Atomic Energy Agency, Tokai, Ibaraki, Japan

⁵ Max-Planck Institut für Astrophysik, Karl-Schwarzschild Strasse 1, D-85748 Garching, Germany

⁶ Istituto Nazionale di Astrofisica, Osservatorio Astronomico di Trieste, Trieste, Italy

⁷ There is a suspicion on whether the GRBs are classical long-duration GRBs (GRB 060505: Amati et al. 2006, and GRB 060614: Gehrels et al. 2006).

A small amount of ⁵⁶Ni ejection has been indicated in the faintness of several Type II SNe (SNe II, e.g., SN 1994W, Sollerman et al. 1998; and SN 1997D, Turatto et al. 1998). The estimated explosion energies, E , of these faint SNe II are very small ($E \lesssim 10^{51}$ ergs, Turatto et al. 1998). These properties are well-reproduced by the *spherical* explosion models that undergo significant fallback if E is sufficiently small (Woosley & Weaver 1995; Iwamoto et al. 2005). Thus these faint SN explosions with low E seem to be superficially irreconcilable to the formation of energetic GRBs (Gal-Yam et al. 2006). However, Nomoto et al. (2006a;⁸ see also Nomoto et al. 2004) has predicted the existence of “dark hypernovae” (i.e., long GRBs with no SNe) based on the argument in the next paragraph. In this Letter, we present actual hydrodynamical models in which a high-energy narrow jet produces a GRB and a faint/dark SN with little ⁵⁶Ni ejection.

An indication that some faint SNe produce high-energy jets is seen in the abundance patterns of the extremely metal-poor (EMP) stars with $[\text{Fe}/\text{H}] < -3.5$.⁹ It has been suggested that the abundance patterns of these EMP stars show the nucleosynthesis yields of a single core-collapse SN (e.g., Beers & Christlieb 2005). In particular, the C-enhanced type of the EMP stars have been well explained by the faint SNe (Umada & Nomoto 2005; Iwamoto et al. 2005; Nomoto et al. 2006b; Tominaga et al. 2007), except for their large Co/Fe and Zn/Fe ratios (e.g., Depagne et al. 2002; Bessell & Christlieb 2005). The enhancement of Co and Zn in low metallicity stars requires explosive nucleosynthesis under high entropy. In a “spherical” model,

⁸ The ppt file is available from “program” at <http://www.merate.mi.astro.it/docM/OAB/Research/SWIFT/sanservolo2006/>

⁹ Here $[A/B] \equiv \log_{10}(N_A/N_B) - \log_{10}(N_A/N_B)_{\odot}$, where the subscript \odot refers to the solar value and N_A and N_B are the abundances of elements A and B, respectively.

a high-entropy explosion corresponds to a high-energy explosion that inevitably synthesizes a large amount of ^{56}Ni . One possible solution to this incompatibility is that some faint SNe are associated with a narrow jet within which a high-entropy region is confined (Umeda & Nomoto 2005). If this would be a realistic model for the EMP stars, some faint SNe would accompany sufficiently energetic jets to produce GRBs.

In this Letter, we present hydrodynamical and nucleosynthetic models of the $40 M_{\odot}$ star explosions with relativistic jets.¹⁰ We show that these models can explain the existence of GRB-HNe and GRBs without bright SNe in a unified manner. We suggest that both GRB-HNe and GRBs without bright SNe are BH-forming SNe involving relativistic jets and that these explosions are responsible for the formation of the EMP stars.

2. MODELS

We investigate the jet-induced explosions (e.g., Maeda & Nomoto 2003; Nagataki et al. 2006) of the $40 M_{\odot}$ Population III stars (Umeda & Nomoto 2005; Tominaga et al. 2007) using a multi-dimensional special relativistic Eulerian hydrodynamic code (Umeda et al. 2005; N. Tominaga, 2007, PhD thesis, in preparation). We assume that the explosions of the $40 M_{\odot}$ Population III stars involve relativistic jets in analogy with the $40 M_{\odot}$ Pop I GRB-HNe, since the Fe core masses of Population III and Population I stars are similar.

We inject the jets at a radius $R_{\text{in}} \sim 900$ km, corresponding to an enclosed mass of $M \sim 1.4 M_{\odot}$, and follow the jet propagation. Since the explosion mechanism of GRB-HNe is still under debate, the jets are treated parametrically with the following five parameters: energy deposition rate (\dot{E}_{dep}), total deposited energy (E_{dep}), initial half angle of the jets (θ_{jet}), initial Lorentz factor (Γ_{jet}), and the ratio of thermal to total deposited energies (f_{th}).

In this Letter, we investigate the dependence of nucleosynthesis outcome on \dot{E}_{dep} for a range of $\dot{E}_{\text{dep},51} \equiv \dot{E}_{\text{dep}}/10^{51} \text{ergs s}^{-1} = 0.3 - 1500$. The diversity of \dot{E}_{dep} is consistent with the wide range of the observed isotropic equivalent γ -ray energies and timescales of GRBs (Amati et al. 2006 and references therein). Variations of activities of the central engines, possibly corresponding to different rotational velocities or magnetic fields, may well produce the variation of \dot{E}_{dep} . We expediently fix the other parameters as $E_{\text{dep}} = 1.5 \times 10^{52} \text{ergs}$, $\theta_{\text{jet}} = 15^{\circ}$, $\Gamma_{\text{jet}} = 100$, and $f_{\text{th}} = 10^{-3}$ in all models.

The thermodynamic history is traced with marker particles representing individual Lagrangian elements (e.g., Maeda & Nomoto 2003). The nucleosynthesis calculation is performed as post-processing and includes 280 species up to ^{79}Br (see Umeda & Nomoto 2005, Table 1). Because recent studies (e.g., Rampp & Janka 2000; Fröhlich et al. 2006) suggest that the electron fraction (Y_e) is affected by neutrino processes, we assume $Y_e = 0.5001$ in the Fe core to maximize the Co/Fe ratio (Umeda & Nomoto 2005).

The thermodynamic history of the jet is also traced

¹⁰ Details of the numerical method, input physics, and the performance of the code will be described in N. Tominaga (2007, PhD thesis, in preparation).

by the marker particles. In computing the jet composition, we assume that the jet expands adiabatically from the Schwartzschild radius to the inner boundary of the computational domain, and that the jet initially has the composition of the accreted stellar materials. The details will be presented in future work.

3. RESULTS

In order to inject the jet, the ram pressure of the jet (P_{jet}) should overcome that of the infalling material (P_{fall}). P_{jet} is determined by R_{in} , \dot{E}_{dep} , θ_{jet} , Γ_{jet} , and f_{th} , thus being constant in time in the present models. On the other hand, P_{fall} decreases with time, since the density of the outer materials decreases following the gravitational collapse (e.g., Fryer & Mészáros 2003). For lower \dot{E}_{dep} , P_{jet} is lower, so that the jet injection ($P_{\text{jet}} > P_{\text{fall}}$) is realized at a later time when the central remnant becomes more massive due to more infall.

After the jet injection is initiated, the shock fronts between the jets and the infalling material proceed outward in the stellar mantle. Figure 1 is a snapshot of the model with $\dot{E}_{\text{dep},51} = 15$ at 1 s after the start of jet injection. When the jet injection ends, the jets have been decelerated by collisions with the dense stellar mantle and the shock has become more spherical. The inner material is ejected along the jet-axis but not along the equatorial plane. On the other hand, the outer material is ejected even along the equatorial plane because the infall along the equatorial plane is terminated as the shock reaches the equatorial plane (e.g., Maeda & Nomoto 2003; Nagataki et al. 2006).

3.1. ^{56}Ni Mass

The top panel of Figure 2 shows the dependence of the ejected $M(^{56}\text{Ni})$ on the energy deposition rate \dot{E}_{dep} . For lower \dot{E}_{dep} , smaller $M(^{56}\text{Ni})$ is synthesized in explosive nucleosynthesis because of lower post-shock densities and temperatures (e.g., Maeda & Nomoto 2003; Nagataki et al. 2006; Maeda & Tominaga 2007, hereafter MT07). While the materials in the C+O layer fall through the inner boundary, P_{fall} decreases only moderately, being almost constant ($P_{\text{fall}} \sim P_{\text{fall}}^{\text{C+O}} \sim 10^{26} \text{dyn cm}^{-2}$) during this phase because of the relatively shallow pre-SN density gradient in the C+O layer (e.g., Fryer & Mészáros 2003; MT07).

If $\dot{E}_{\text{dep},51} \gtrsim 3$, $P_{\text{jet}} > P_{\text{fall}}^{\text{C+O}}$ so that the jet injection is initiated below the bottom of the C+O layer, leading to the synthesis of $M(^{56}\text{Ni}) \gtrsim 10^{-3} M_{\odot}$. If $\dot{E}_{\text{dep},51} < 3$, on the other hand, $P_{\text{jet}} < P_{\text{fall}}^{\text{C+O}}$ so that the jet injection is delayed until P_{fall} decreases below P_{jet} and initiated near the surface of the C+O core; then the ejected ^{56}Ni is as small as $M(^{56}\text{Ni}) < 10^{-3} M_{\odot}$.

^{56}Ni contained in the relativistic jets is only $M(^{56}\text{Ni}) \sim 10^{-6}$ to $10^{-4} M_{\odot}$ because the total mass of the jets is $M_{\text{jet}} \sim 10^{-4} M_{\odot}$ in our model with $\Gamma_{\text{jet}} = 100$ and $E_{\text{dep}} = 1.5 \times 10^{52} \text{ergs}$. The ^{56}Ni production in the jets is predominant only for $\dot{E}_{\text{dep},51} < 1.5$ in the present model (Fig. 2). The models cannot synthesize ^{56}Ni explosively and eject very little $M(^{56}\text{Ni}) (\sim 10^{-6} M_{\odot})$.

3.1.1. GRB-HNe

For high energy deposition rates ($\dot{E}_{\text{dep},51} \gtrsim 60$), the explosions synthesize large $M(^{56}\text{Ni})$ ($\gtrsim 0.1M_{\odot}$) being consistent with GRB-HNe. The remnant mass was $M \sim 1.4M_{\odot}$ when the jet injection was started, but it grows as material is accreted from the equatorial plane. The final BH masses range from $M_{\text{BH}} = 10.8M_{\odot}$ for $\dot{E}_{\text{dep},51} = 60$ to $M_{\text{BH}} = 5.5M_{\odot}$ for $\dot{E}_{\text{dep},51} = 1500$, which are consistent with the masses of stellar-mass BHs (Bailyn et al. 1998). The model with $\dot{E}_{\text{dep},51} = 300$ synthesizes $M(^{56}\text{Ni}) \sim 0.4M_{\odot}$ and results in $M_{\text{BH}} = 6.4M_{\odot}$.

Since the jet injection with large \dot{E}_{dep} is in short timescale and terminated before the jets reach the surface of the C+O core, the asphericity of the ejecta inside the C+O core for $\dot{E}_{\text{dep},51} \gtrsim 60$ is probably consistent with a relatively oval explosion as indicated by the light curve and spectra of GRB-HNe (Maeda et al. 2006a,b).

Neutrino annihilation has been estimated to provide only a small energy deposition rate (e.g., $\dot{E}_{\text{dep},51} \sim 1$; Woosley 1993), leading to the synthesis of smaller $M(^{56}\text{Ni})$ than is required for GRB-HNe. In order to synthesize a sufficient amount of ^{56}Ni , large \dot{E}_{dep} should be produced via some mechanism, e.g., magneto-rotation (Mizuno et al. 2004; another possibility, ^{56}Ni production in the disk wind, is discussed in MT07).

3.1.2. GRBs 060505 and 060614

For low energy deposition rates ($\dot{E}_{\text{dep},51} < 3$), the ejected ^{56}Ni masses [$M(^{56}\text{Ni}) < 10^{-3}M_{\odot}$] are smaller than the upper limits for GRBs 060505 and 060614. The final BH masses range from $M_{\text{BH}} = 18.2M_{\odot}$ for $\dot{E}_{\text{dep},51} = 0.3$ to $M_{\text{BH}} = 15.1M_{\odot}$ for $\dot{E}_{\text{dep},51} = 3$. While the material ejected along the jet direction involves those from the C+O core, the material along the equatorial plane is ejected only from the outer part of the H envelope. Thus M_{BH} exceeds the C+O core mass $M_{\text{C+O}} = 13.9M_{\odot}$ for the $40M_{\odot}$ star.

If the star lost the H and He envelopes before its core collapsed, and if the explosion is viewed from the jet direction, we would observe GRB without SN re-brightening. This may be the situation for GRBs 060505 and 060614.

3.1.3. GRBs with Faint or Subluminous SNe

For intermediate energy deposition rates ($3 \lesssim \dot{E}_{\text{dep},51} < 60$), the explosions eject $10^{-3}M_{\odot} \lesssim M(^{56}\text{Ni}) < 0.1M_{\odot}$ and the final BH masses are $10.8M_{\odot} \lesssim M_{\text{BH}} < 15.1M_{\odot}$. The resulting SN is faint [$M(^{56}\text{Ni}) < 0.01M_{\odot}$] or sub-luminous [$0.01M_{\odot} \lesssim M(^{56}\text{Ni}) < 0.1M_{\odot}$].

Nearby GRBs with faint or sub-luminous SNe have not been observed. Possible reasons may be that (1) they do not occur intrinsically, i.e., the energy deposition rate is bimodally distributed, or that (2) the number of observed nearby GRBs is still too small. For case 1, the GRB progenitors may be divided into two groups, e.g., with rapid or slow rotation and/or with strong or weak magnetic fields. For case 2, future observations will detect GRBs associated with a faint or sub-luminous SN.

3.2. Abundance Ratio: C/Fe

The bottom panel of Figure 2 shows the dependence of the abundance ratio [C/Fe] on \dot{E}_{dep} . Lower \dot{E}_{dep} yields larger M_{BH} and thus larger [C/Fe], because the infall decreases the amount of inner core material (Fe) relative to that of outer material (C) (see also Maeda & Nomoto 2003). As in the case of $M(^{56}\text{Ni})$ (§3.1), [C/Fe] changes dramatically at $\dot{E}_{\text{dep},51} \sim 3$.

The abundance patterns of the EMP stars are good indicators of nucleosynthesis in a single SN because the Galaxy was effectively unmixed at $[\text{Fe}/\text{H}] < -3$ (e.g., Tumlinson 2006). They are classified into three groups according to [C/Fe]: (1) [C/Fe] ~ 0 , normal EMP stars ($-4 < [\text{Fe}/\text{H}] < -3$, e.g., Cayrel et al. 2004); (2) [C/Fe] $\gtrsim +1$, Carbon-enhanced EMP (CEMP) stars ($-4 < [\text{Fe}/\text{H}] < -3$, e.g., CS 22949-37; Depagne et al. 2002); (3) [C/Fe] $\sim +4$, hyper metal-poor (HMP) stars ($[\text{Fe}/\text{H}] < -5$, e.g., HE 0107-5240; Christlieb et al. 2002; Bessell & Christlieb 2005; HE 1327-2326, Frebel et al. 2005).

Figure 3 shows that the general abundance patterns of the normal EMP stars, the CEMP star CS 22949-37, and the HMP stars HE 0107-5240 and HE 1327-2326 are reproduced by models with $\dot{E}_{\text{dep},51} = 120, 3.0, 1.5,$ and 0.5 , respectively (see Table 1 for model parameters). The model for the normal EMP stars ejects $M(^{56}\text{Ni}) \sim 0.2M_{\odot}$, i.e. a factor of 2 less than SN 1998bw. On the other hand, the models for the CEMP and the HMP stars eject $M(^{56}\text{Ni}) \sim 8 \times 10^{-4}$ and $4 \times 10^{-6}M_{\odot}$, respectively, which are always smaller than the upper limits for GRBs 060505 and 060614. The lack of the metal-poor stars at $-5 < [\text{Fe}/\text{H}] < -4$ is explained by the narrow range of \dot{E}_{dep} . The N/C ratio in the models for CS 22949-37 and HE 1327-2326 is enhanced by partial mixing between the He and H layers during pre-SN evolution (Iwamoto et al. 2005).

4. DISCUSSION AND CONCLUSION

We have computed hydrodynamics and nucleosynthesis for the explosions induced by relativistic jets. We have shown that (1) the explosions with large \dot{E}_{dep} are observed as GRB-HNe and their yields explain the abundances of normal EMP stars, and (2) the explosions with small \dot{E}_{dep} are observed as GRBs without bright SNe and are responsible for the formation of the CEMP and the HMP stars. We thus propose that GRB-HNe and GRBs without bright SNe belong to a continuous series of BH-forming SNe with the relativistic jets of different \dot{E}_{dep} .

Presently, the number fraction of GRBs without bright SNe relative to the known nearby GRBs is $\sim 40\%$ (e.g., Woosley & Bloom 2006). On the other hand, among the EMP stars with $[\text{Fe}/\text{H}] < -3.5$, the fractions of the CEMP and the HMP stars relative to the EMP stars are $\sim 25\%$ and $\sim 15\%$, respectively (Beers & Christlieb 2005). Although the numbers of observed GRBs and the EMP stars with $[\text{Fe}/\text{H}] < -3.5$ are still too small to discuss statistics, the fraction of GRBs without bright SNe is consistent with the sum of the fractions of the CEMP and the HMP stars. Thus GRBs 060505 and 060614 are likely related to the CEMP stars ejecting $M(^{56}\text{Ni}) \sim 10^{-4}$ to $10^{-3}M_{\odot}$ or HMP stars ejecting $M(^{56}\text{Ni}) \sim 10^{-6}M_{\odot}$.

A short GRB, probably the result of the merger of two compact objects (e.g., Gehrels et al. 2005), synthesizes

TABLE 1
 MODELS COMPARED WITH METAL-POOR STARS.

Stars	\dot{E}_{dep} [10^{51} ergs s^{-1}]	$M(^{56}\text{Ni})$ [M_{\odot}]	M_{BH} [M_{\odot}]	[C/Fe]
EMP	120	2.09×10^{-1}	9.1	0.02
CS 22949–37	3.0	7.64×10^{-4}	15.1	1.20
HE 1327–2326	1.5	3.90×10^{-6}	16.9	3.21
HE 0107–5240	0.5	2.80×10^{-6}	17.1	3.91

virtually no ^{56}Ni because the ejecta must be too neutron-rich. In contrast, our model suggests that GRBs 060505 and 060614 produced $M(^{56}\text{Ni}) \sim 10^{-4} - 10^{-3} M_{\odot}$ or $\sim 10^{-6} M_{\odot}$. If such a GRB without a bright SN occurs

in a very faint and nearby galaxy, our model predicts that some re-brightening due to the ^{56}Ni decay can be observed.

REFERENCES

- Amati, L., Della Valle, M., Frontera, F., Malesani, D., Guidorzi, C., Montanari, E., & Pian, E. 2006, A&A, submitted (astro-ph/0607148)
- Bailyn, C.D., Jain, R.K., Coppi, P., & Orosz, J.A. 1998, ApJ, 499, 367
- Beers, T.C., & Christlieb, N. 2005, ARA&A, 43, 531
- Bessell, M. S., & Christlieb, N. 2005, in IAU Symp. 228, From Lithium to Uranium: Elemental Tracers of Early Cosmic Evolution, ed. V. Hill et al. (Cambridge: Cambridge Univ. Press), 237
- Cayrel, R., et al. 2004, A&A, 416, 1117
- Christlieb, N., et al. 2002, Nature, 419, 904
- Della Valle, M., et al. 2006, Nature, 444, 1050
- Depagne, E., et al. 2002, A&A, 390, 187
- Frebel, A., et al. 2005, Nature, 434, 871
- Fröhlich, C., et al. 2006, ApJ, 637, 415
- Fryer, C., & Mészáros, P. 2003, ApJ, 588, L25
- Fynbo, J.P.U., et al. 2006, Nature, 444, 1047
- Galama, T. J., et al. 1998, Nature, 395, 670
- Gal-Yam, A., et al. 2006, Nature, 444, 1053
- Gehrels, N., et al. 2005, Nature, 437, 851
- Gehrels, N., et al. 2006, Nature, 444, 1044
- Hjorth, J., et al. 2003, Nature, 423, 847
- Iwamoto, N., Umeda, H., Tominaga, N., Nomoto, K., & Maeda, K. 2005, Science, 309, 451
- Iwamoto, K., et al. 1998, Nature, 395, 672
- Maeda, K., Mazzali, P. A., & Nomoto, K. 2006a, ApJ, 645, 1331
- Maeda, K., & Nomoto, K. 2003, ApJ, 598, 1163
- Maeda, K., Nomoto, K., Mazzali, P. A., & Deng, J. 2006b, ApJ, 640, 854
- Maeda, K., & Tominaga, N. 2007, ApJ, submitted (MT07)
- Malesani, D., et al. 2004, ApJ, 609, L5
- Mazzali, P. A., et al. 2006, ApJ, 645, 1323
- Mizuno, Y., Yamada, S., Koide, S., & Shibata, K. 2004, ApJ, 615, 389
- Nagataki, S., Mizuta, A., & Sato, K. 2006, ApJ, 647, 1255
- Nomoto, K., Maeda, K., Mazzali, P. A., Umeda, H., Deng, J., & Iwamoto, K. 2004, in Stellar Collapse, ed. C. L. Fryer (Dordrecht: Kluwer), 277 (astro-ph/0308136)
- Nomoto, K., Tominaga, N., Tanaka, M., Maeda, K., Suzuki, T., Deng, J.S., Mazzali, P.A. 2006a, in *Swift* and GRBs: Unveiling the Relativistic Universe, ed. G. Chincarini et al. (Bologna: Italian Physical Society), in press (astro-ph/0702472)
- Nomoto, K., Tominaga, N., Umeda, H., Kobayashi, C., & Maeda, K. 2006b, Nucl. Phys. A, 777, 424 (astro-ph/0605725)
- Rampp, M., & Janka, H.-Th. 2000, ApJ, 539, L33
- Sollerman, J., Cumming, R.J., & Lundqvist, P. 1998, ApJ, 493, 933
- Stanek, K. Z., et al. 2003, ApJ, 591, L17
- Tominaga, N., Umeda, H., & Nomoto, K. 2007, ApJ, 660, in press (astro-ph/0701381)
- Tumlinson, J. 2006, ApJ, 641, 1
- Turatto, M., et al. 1998, ApJ, 498, L129
- Umeda, H., & Nomoto, K. 2005, ApJ, 619, 427
- Umeda, H., Tominaga, N., Maeda, K., & Nomoto, K. 2005, ApJ, 633, L17
- Woosley, S. E. 1993, ApJ, 405, 273
- Woosley, S. E., & Bloom, J.S. 2006, ARA&A, 44, 507
- Woosley, S. E., & Weaver, T. A. 1995, ApJS, 101, 181

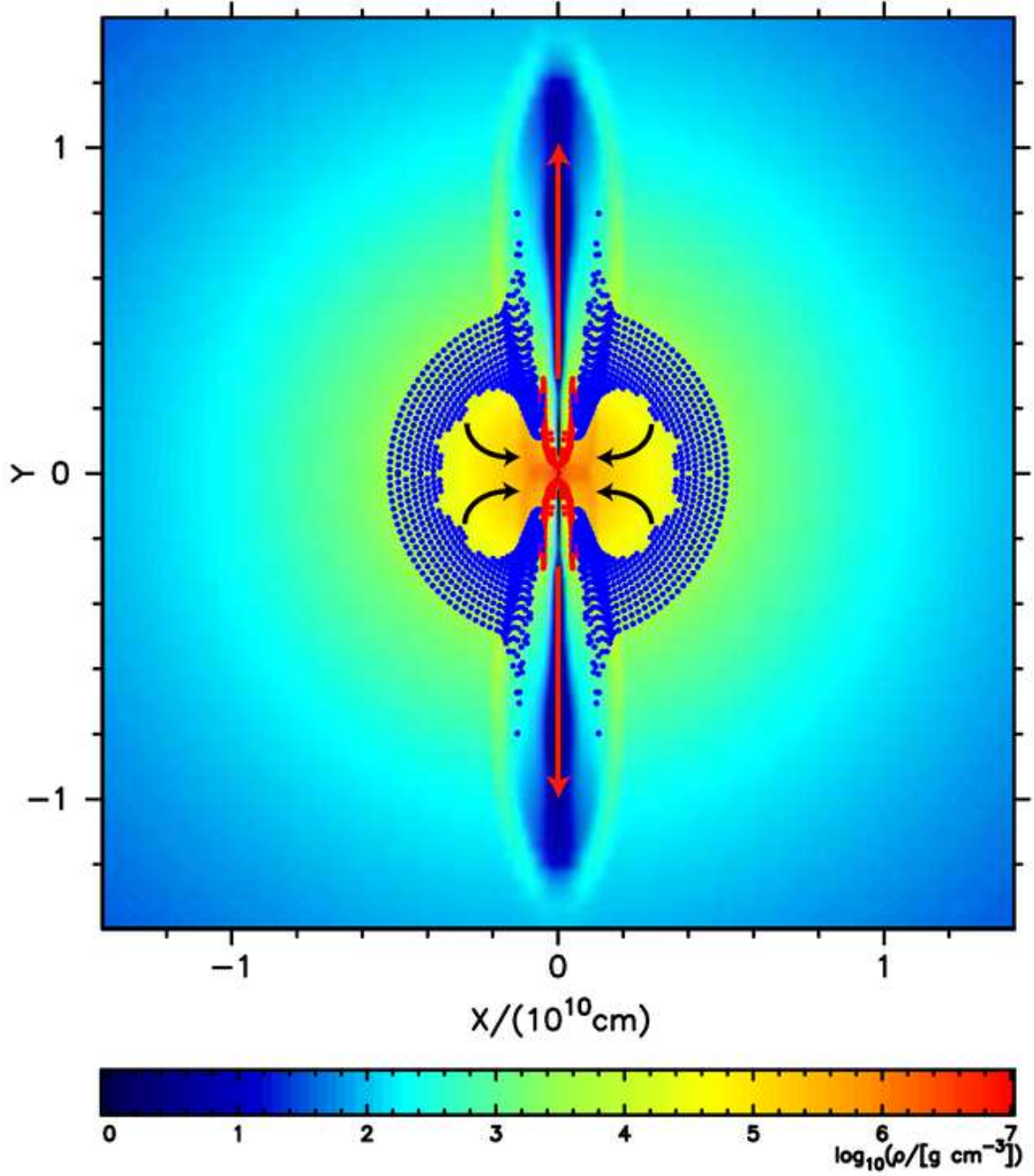


FIG. 1.— Density structure of the $40 M_{\odot}$ Population III star explosion model of $\dot{E}_{\text{dep},51} = 15$ at 1 s after the start of the jet injection. The jets penetrate the stellar mantle (*red arrows*) and material falls on the plane perpendicular to the jets (*black arrows*). The dots represent ejected Lagrangian elements dominated by Fe (^{56}Ni , *red*) and by O (*blue*).

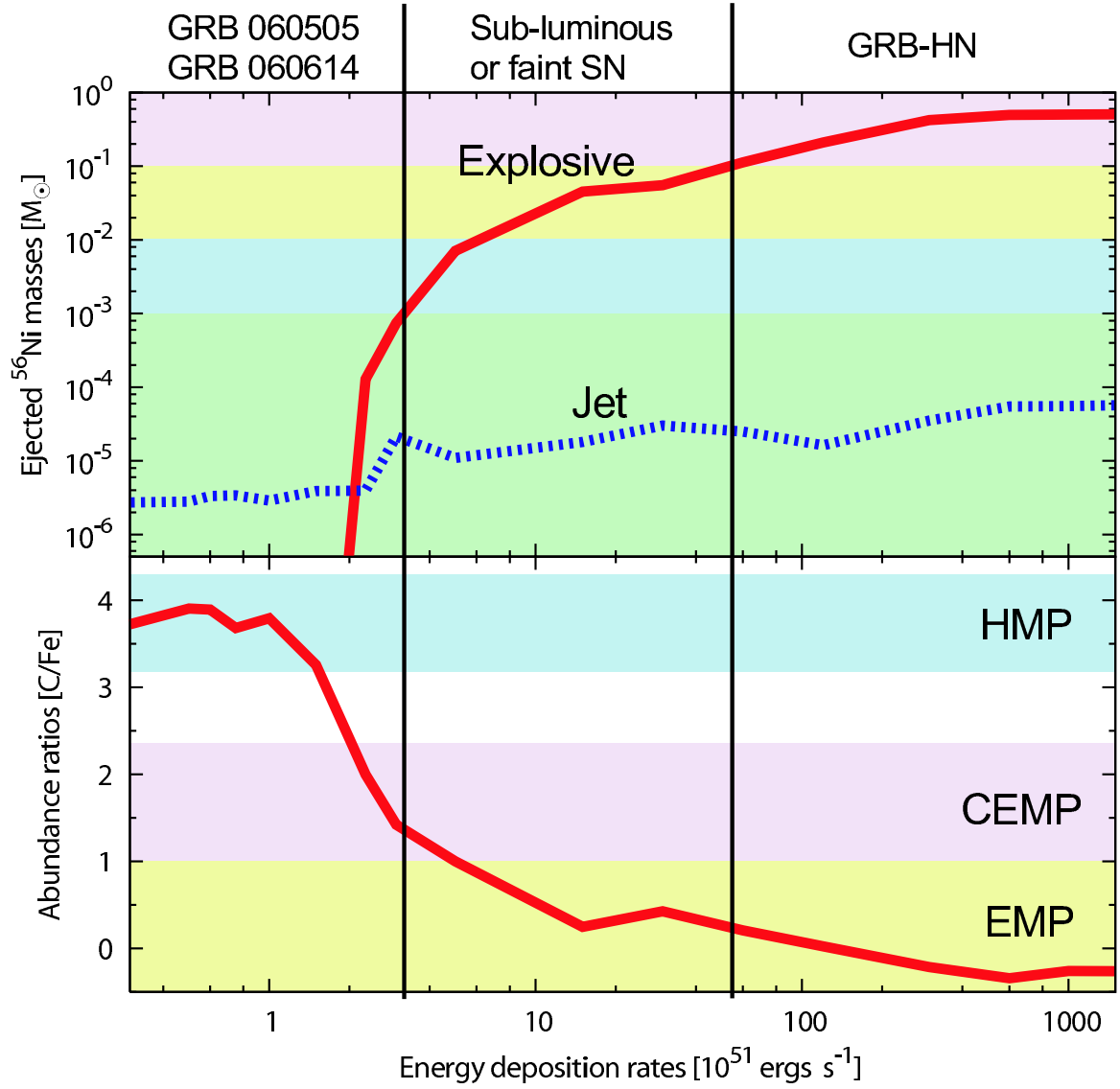


FIG. 2.— *Top*: Ejected ^{56}Ni mass (*red*: explosive nucleosynthesis products, *blue*: the jet contribution) as a function of the energy deposition rate. The background color shows the corresponding SNe (*red*: GRB-HNe, *yellow*: sub-luminous SNe, *blue*: faint SNe, *green*: GRBs 060505 and 060614). Vertical lines divide the resulting SNe according to their brightness. *Bottom*: Dependence of abundance ratio $[\text{C}/\text{Fe}]$ on the energy deposition rate. The background color shows the corresponding metal-poor stars (*yellow*: EMP, *red*: CEMP, *blue*: HMP stars).

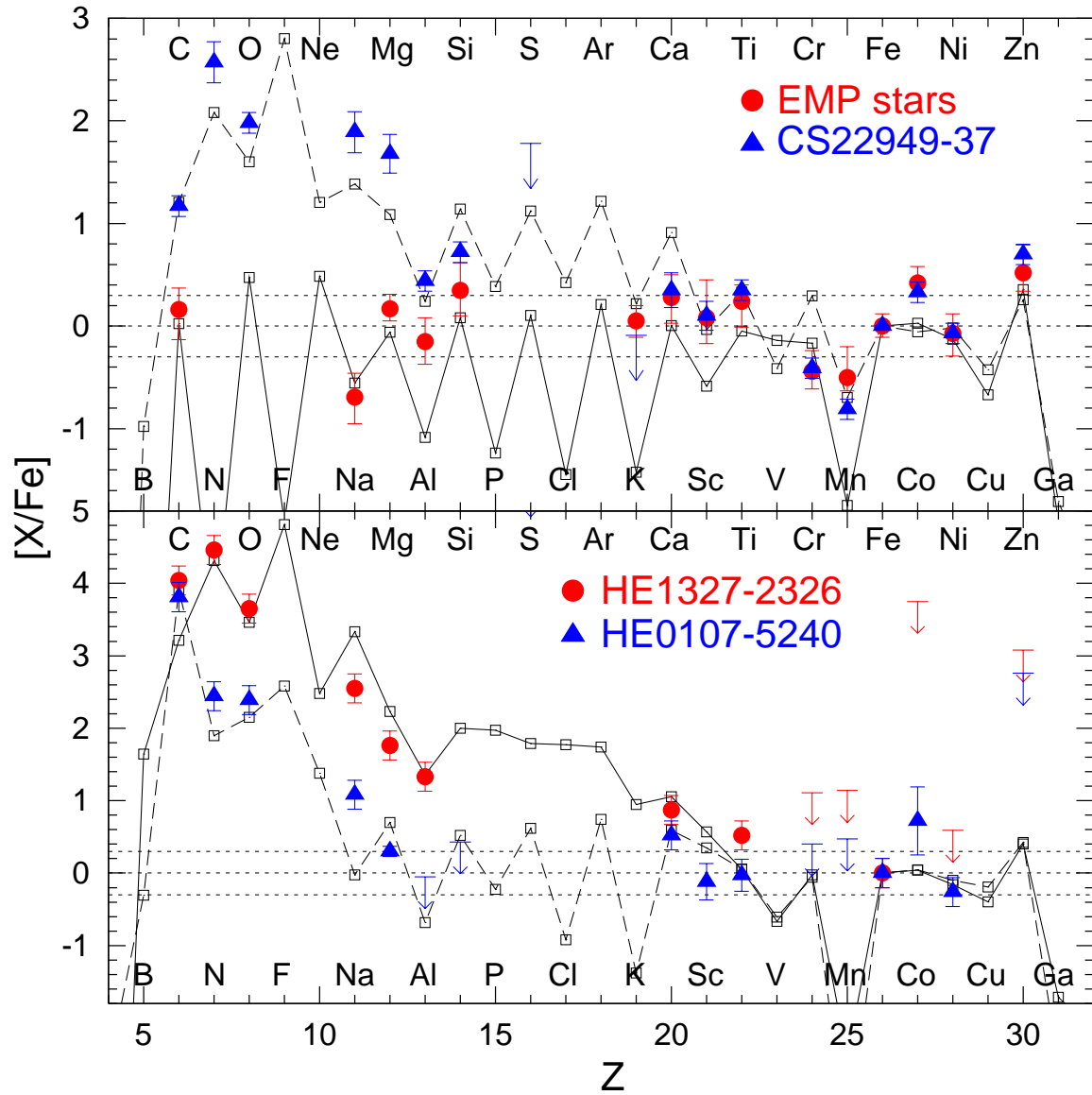


FIG. 3.— Comparison of the abundance patterns of metal-poor stars and of models. *Top*: Normal EMP (red dots) and CEMP (blue triangles) stars and models with $\dot{E}_{\text{dep},51} = 120$ (solid line) and $= 3.0$ (dashed line). *Bottom*: HMP stars: HE 1327–2326, (red dots), and HE 0107–5240, (blue triangles) and models with $\dot{E}_{\text{dep},51} = 1.5$ (solid line) and $= 0.5$ (dashed line).